ISSN 0030-400X, Optics and Spectroscopy, 2018, Vol. 124, No. 3, pp. 343–348. © Pleiades Publishing, Ltd., 2018.
Original Russian Text © A.S. Abramov, I.O. Zolotovskii, D.A. Korobko, A.A. Fotiadi, 2018, published in Optika i Spektroskopiya, 2018, Vol. 124, No. 3, pp. 342–347.

NONLINEAR AND QUANTUM OPTICS

A Fiber-Optic System Generating Pulses of High Spectral Density

A. S. Abramov[a], I. O. Zolotovskii[a], D. A. Korobko[a,]*, and A. A. Fotiadi[a, b]

[a] *Ulyanovsk State University, Ulyanovsk, 432017 Russia*

[b] *Université de Mons, B7000 Mons, Belgium*

**e-mail: korobkotam@rambler.ru*

Received October 17, 2017

Abstract—A cascade fiber-optic system that generates pulses of high spectral density by using the effect of nonlinear spectral compression is proposed. It is demonstrated that the shape of the pulse envelope substantially influences the degree of compression of its spectrum. In so doing, maximum compression is achieved for parabolic pulses. The cascade system includes an optical fiber exhibiting normal dispersion that decreases along the fiber length, thereby ensuring that the pulse envelope evolves toward a parabolic shape, along with diffraction gratings and a fiber spectral compressor. Based on computer simulation, we determined parameters of cascade elements leading to maximum spectral density of radiation originating from a subpicosecond laser pulse of medium energy.

DOI: 10.1134/S0030400X18030037

INTRODUCTION

The development of laser systems generating radiation of high spectral density is topical, because it has a number of important applications, e.g., generation of harmonics and frequency conversion in nonlinear media [1, 2], efficient signal amplification in an active resonance medium, and resonance irradiation of the medium (for instance, for isotope separation [3, 4]). This high practical importance makes the development of fiber sources of radiation of high spectral density a high priority. Small size, reliability, and high beam quality make systems based on optical fibers extremely attractive for applications. However, fiber-laser sources of high spectral purity are usually characterized by a relatively low power [5], while nonlinear processes developing in fibers in the course of amplification lead to considerable spectral broadening [6]. In the present work, we propose an alternative approach based on nonlinear spectral compression (SC) of high-power pulsed radiation of a fiber laser, which allows obtaining pulses of high spectral brightness.

Nonlinear SC is a well-known effect that takes place due to self-phase modulation (SPM) of a negatively chirped laser pulse propagating in a nonlinear optical waveguide [7, 8]. This effect consists in SPM nearly completely compensating the negative chirp at a certain propagation length in a fiber. In so doing, the width of the pulse spectrum attains a minimum. When developing a fiber generator of radiation of high spectral density, we propose using a standard subpicosecond pulsed fiber laser as a source of radiation that will subsequently undergo spectral compression. The recent development of fiber lasers allows using sources of different spectral ranges (1050, 1550, 1950 nm, etc.) with pulse durations of about 0.2–1 ps and pulse energies exceeding 1 nJ [9, 10] for spectral compression. Here, we propose a scheme of an SC of such pulses suitable for any spectral range corresponding to fiber-laser radiation, which allows reaching a high level of spectral brightness required for applications.

1. MODEL OF A FIBER SPECTRAL COMPRESSOR

Let us analyze pulse propagation in a nonlinear fiber by using the nonlinear Schrödinger equation (NSE) governing complex amplitude $A(z,t)$ [11] that has the form

$$\frac{\partial A}{\partial z} - \frac{i\beta_2}{2}\frac{\partial^2 A}{\partial t^2} + i\gamma|A|^2 A = 0. \quad (1)$$

Here, z is the longitudinal coordinate, t is the time in the retarded coordinate system, β_2 is the group-velocity dispersion (GVD) of the fiber, and γ is the parameter of Kerr nonlinearity. For the sake of simplicity and clarity of our analysis, let us neglect losses in the fiber and wavelength dependence of β_2, i.e., the contributions of third and higher orders of dispersion. This approach can be used if the fiber length is much shorter than $L_{3D} = 2\tau^3/\beta_3$, where τ is the width of the

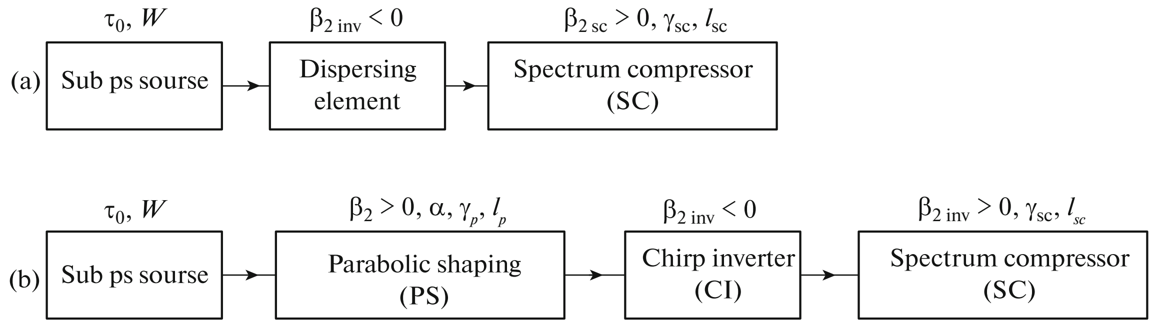

Fig. 1. The scheme for spectral compression of laser pulses ((a) without a *PS* element, (b) with a *PS* element).

pulse at the input of the spectral compressor and β_3 is the third-order dispersion coefficient. This condition is fulfilled for pulses with a duration of 10 ps and longer that propagate in optical fibers shorter than 1000 m and are characterized by $\beta_3 < 10^{-1}$ ps^3/m. It is this situation that is realized in our case.

Several schemes of systems for spectral compression of laser pulses are presented in Fig. 1. The same figure also shows the corresponding notations for parameters of group-velocity dispersion β_2 and nonlinearity γ that characterize each system element. In a standard SC scheme (Fig. 1a), a pulse that lacks frequency modulation initially propagates through a linear dispersing element, where it acquires a negative linear chirp. This process can be most effectively accomplished by using a pair of diffraction gratings. The pulse envelope after propagation through this element can be expressed in the form

$$A(0,t) = a(t)\exp(iCt^2), \quad (2)$$

where $C < 0$ is the rate of frequency modulation. At the next and last stage, a pulse exhibiting negative frequency modulation is injected into a nonlinear fiber. In the course of propagation, the pulse experiences SPM that imparts spectral modulation to the pulse opposite to the original one; i.e., the phase of the pulse acquires an additional term proportional to propagation length $z - \gamma|a|^2 z$. As a result, frequency modulation of the pulse becomes rather complex, its form depending on the shape of the pulse envelope, initial frequency modulation, and propagation length:

$$\varphi(t) = Ct^2 - \gamma|a|^2 z.$$

The spectral width of the pulse exhibiting high frequency modulation is $\sim\varphi'(t)$. At a certain length of the fiber, the width of the frequency spectrum reaches a minimum due to compensation of the negative chirp; i.e., spectral compression of the pulse is achieved. Obviously, the quality of compression depends on the shape of envelope $a(t)$. It can be shown that a parabolic shape of the pulse envelope,

$$a(t) = \sqrt{P_0\left(1 - \frac{t^2}{\tau_p^2}\right)}, \quad |t| \le \tau_p, \quad a = 0, \quad |t| > \tau_p \quad (3)$$

gives the best results [12, 13], where P_0 is the peak power. Indeed, in the dispersionless approximation, $\beta_2 = 0$, frequency modulation at certain length $z = L$ can be completely compensated:

$$\varphi(t) = C_0 t^2 - \gamma P_0\left(1 - \frac{t^2}{\tau_p^2}\right)L = -\gamma P_0 L = \text{const};$$

i.e., the pulse becomes transform-limited: $\varphi'(t) \equiv 0$. In so doing, a minimal spectral width is achieved. In the approximation of the standard variation method, in which the pulse envelope retains its shape upon propagation, the influence of GVD on SC length can be found relatively straightforwardly [14]. The results show that SC develops considerably faster in fibers with normal GVD. As a result of simultaneous temporal compression of the pulse, its minimal spectral width $\Delta\Omega_{min}$ that can be achieved upon compression in a fiber with normal GVD is somewhat larger than the value of $\Delta\Omega_{min}$ obtained in the dispersionless case (at $\beta_2 = 0$).

Note that, in contrast to the case of a parabolic pulse envelope, spectral compression of laser pulses with a different shape, e.g., Gaussian, is accompanied by the appearance of distortions: SPM compensates the initial chirp only partially or locally, which leads to the appearance of wings and/or a pedestal in the compressed-pulse spectrum, thereby reducing efficiency of the process. Based on the above discussion, we propose modifying the scheme of standard SC by incorporating an additional *PS* (parabolic shaping) element into it that will ensure a smooth transformation of the initial shape of the pulse envelope to parabolic (Fig. 1b). This goal can be achieved by, e.g., using modern optical-processing technologies, i.e., forming a pulse with required shape of its envelope and frequency modulation. Programmable phase masks based on liquid crystals or programmable acoustooptic filters can play the role of such elements [15]. However, using such complex and expensive elements is

Table 1. Parameters of pulses and scheme elements

No.	1			2				3	4		
Element	Source of radiation			Fiber exhibiting gradually decreasing dispersion and constant nonlinearity				Diffraction gratings	Fiber exhibiting constant dispersion and nonlinearity		
Stage	Coupling of radiation			Parametric shaping of envelope				Chirp inversion	Spectral compression		
Parameters	τ_0, ps	Peak power, W	Initial chirp, C_0, s^{-2}	β_{20}, ps^2/km	α, m^{-1}	γ_p, $(W\,km)^{-1}$	l_p, m	β_{2inv}, ps^2	β_{2sc}, ps^2/km	γ_{sc}, $(W\,km)^{-1}$	l_{sc}, m
Values	0.2	3600	0	84	0.5	3	100	−0.22	5	7	225

not obligatory. It is well known that a pulse acquires a parabolic envelope profile upon propagation in a nonlinear fiber exhibiting hyperbolically decreasing normal dispersion [16]. This effect is related to the fact that, due to relative growth of the influence of nonlinearity, pulse propagation in an optical fiber with decreasing normal GVD is equivalent to pulse propagation in a gain medium with an unlimited gain bandwidth. As a result, a linearly chirped parabolic similariton pulse (i.e., a pulse changing self-similarly) is formed [17]. Technologically, optical fibers with varying GVD and simultaneously constant nonlinearity parameter γ can be fabricated, e.g., on the basis of fibers with a W-shaped refractive-index profile in cross section. When drawing fibers, substantial variation of GVD can be achieved by small variation of fiber diameter. In so doing, mode area and coefficient of nonlinearity along such a fiber can be considered constant with high degree of accuracy [18]. Complementing the system by such an element allows re-shaping the pulse envelope and improving the SC quality at the final stage.

2. NUMERICAL ANALYSIS

In this section, we will present the results of computer simulation of the proposed SC systems. A transform-limited Gaussian pulse of subpicosecond duration was used as an input pulse. Characteristics of the pulse at the input of the cascade scheme, along with dispersion and nonlinear parameters of system elements, are presented in Table 1.

The scheme of spectral compression of the input Gaussian pulse in a traditional scheme (Fig. 1a) is illustrated in Fig. 2a. At the first stage, the pulse acquires a negative chirp. After that, the pulse is injected into an *SC* element in which nonlinear spectral compression takes place. Note that compressed spectrum reveals characteristic wings accompanying the main peak, which are caused by the differences in the initial shape of the pulse envelope. As a result, the final spectral density is low (see Fig. 5 below).

For comparison, evolution of spectrum of the pulse envelope upon pulse propagation along a modified fiber cascade is presented in Fig. 2b. The boundary between the element responsible for parabolic shaping of the pulse envelope (the *PS* element) and spectral compressor (the *SC* element) represented by optical fibers characterized by different parameters of dispersion and nonlinearity is shown by a dashed line. Upon pulse propagation through the *PS* element, its spectrum experiences gradual broadening, so that the shape of the pulse envelope approaches parabolic at fiber length l_p = 100 m. In the process, the spectral density decreases by nearly a factor of 4, while peak power of the pulse decreases by more than a factor of 50 (Fig. 3). A thus-prepared pulse passes through diffraction gratings, which invert its chirp. After that, spectral compression of the pulse takes place in an *SC* fiber element characterized by constant normal dispersion due to gradual compensation of negative frequency modulation. For chosen parameters, maximum spectral compression takes place in a fiber of length l_{sc} = 225 m. Numerical estimates and more detailed description of each of the elements will be given below.

2.1. The PS Element

A subpicosecond pulse with a Gaussian envelope

$$A(\tau) = A_0 \exp\left[-\frac{1}{2}\left(\frac{t}{\tau_0}\right)^2\right], \quad \tilde{A}(\omega) = \frac{1}{2\pi}\int_{-\infty}^{\infty} A(t) e^{-i\omega t} dt$$

arrives at the input of the first element of the discussed fiber system from the source of radiation. The initial pulse duration is τ_0 = 0.2 ps, the peak power at the input is $|A_0|^2$ = 3600 W, and the pulse is initially free from frequency modulation.

The *PS* element consists of a piece of fiber characterized by constant coefficient of nonlinearity γ_p. The normal dispersion in this section of the system decreases according to hyperbolic law of the form $\beta_2(z) = \beta_{20}/(1+\alpha z)$. Here, β_{20} is the initial value of

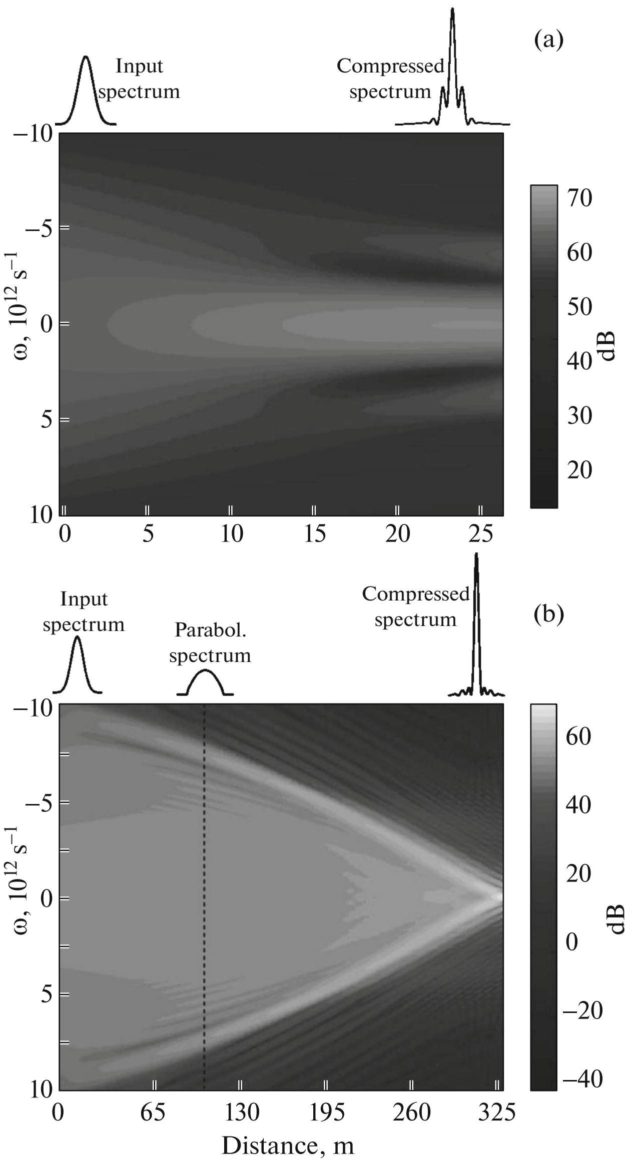

Fig. 2. Evolution of spectrum of a Gaussian pulse in (a) fiber cascade schemes without a *PS* element and (b) in schemes containing it. Changes in the envelope of the pulse spectrum upon pulse propagation through different stages of the cascade are shown schematically.

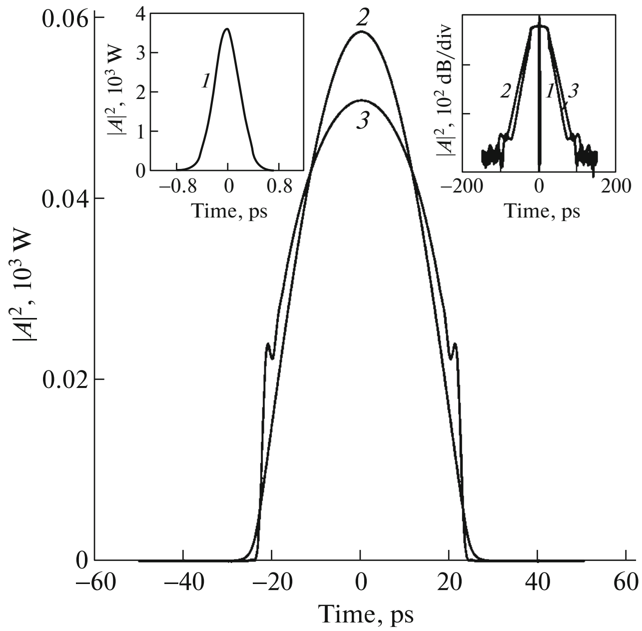

Fig. 3. Temporal profiles of the input pulse (curve *1*), pulse propagated through the stage of parabolic shaping (curve *2*), and pulse with inverted chirp (curve *3*).

dispersion at the input of the element and α is the rate at which the dispersion decreases with distance. Computer simulation of evolution of the pulse envelope was conducted within the framework of the standard stepwise iterative Fourier transform method consisting in consecutive calculation of dispersion and nonlinearity in each separate small section of the fiber [11]. As we mentioned before, dispersion broadening of the pulse is observed at the output of the *PS* element. In the process, its spectrum experiences nonlinear broadening. The pulse envelope approaches a parabolic shape. Correspondingly, frequency modulation (chirp) becomes linear (Figs. 3, 4, curves *2*).

2.2. Chirp Inverter, the CI element

Parabolic shaping is followed by a stage in which the pulse acquires negative frequency modulation (chirp inversion). In the proposed scheme, this operation is implemented by a pair of diffraction gratings, which introduces anomalous dispersion. In so doing, the value of dispersion $\beta_{2\,\mathrm{inv}}$ is chosen so that the temporal profile of the pulse envelope formed after the parabolic shaping stage is preserved as much as possible, while its width at half-maximum remains constant (Fig. 2, curves *2*, *3*):

$$\tilde{A}_{\mathrm{inv}}(z,\omega) = \tilde{A}(z,\omega)\exp\left(\frac{i}{2}\beta_{2\mathrm{inv}}\omega^2\right).$$

2.3. The SC Element

The last and main element (the *SC* element) of the proposed scheme is a fiber in which negative frequency dispersion is compensated due to the effect of self-phase modulation. The length of this section of the fiber is l_{sc}, while normal group-velocity dispersion $\beta_{2\mathrm{sc}}$ and nonlinearity γ_{sc} are constant along the fiber length. Numerical calculation of evolution of the pulse envelope was also conducted by the stepwise iterative Fourier transform method. The pulse spectrum is shown in Fig. 5 (curve *3*) after its propagation through all stages (the *PS* and *SC* elements). For comparison, the initial spectrum of the Gaussian pulse (curve *1*) and compressed spectrum obtained in the standard scheme (without the parabolic shaping stage) (curve *2*) are also shown. Note that spectral compres-

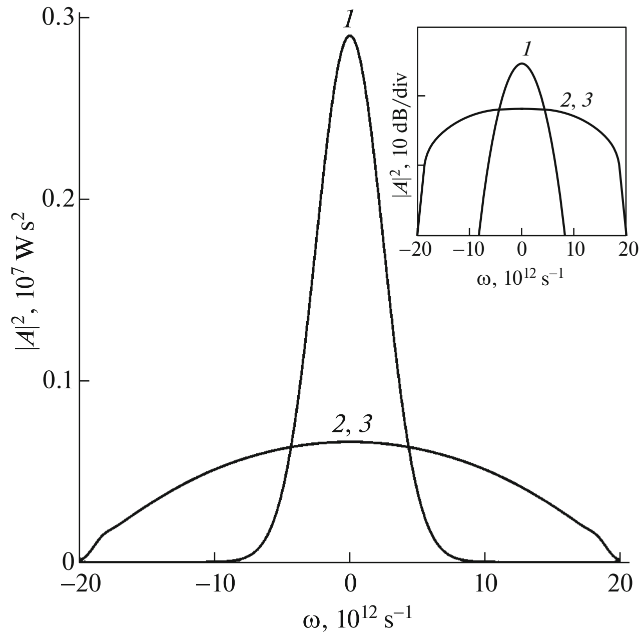

Fig. 4. Spectra of the input pulse (curve *1*) and pulse spectra after the stages of parabolic shaping and chirp inversion (curves *2*, *3*, respectively). The same spectra are shown on a logarithmic scale in the inset.

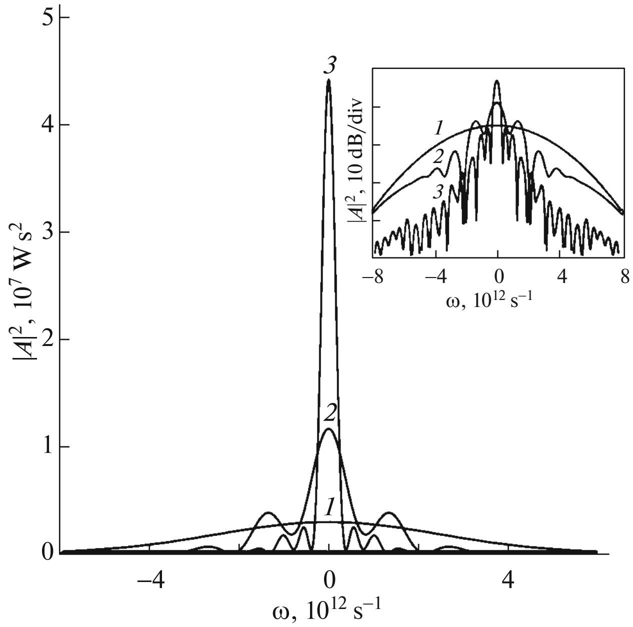

Fig. 5. Spectrum of the input pulse (curve *1*), output spectra of the pulse in cascade without PS element (curve *2*) and with PS element (curve *3*). The same spectra are shown on a logarithmic scale in the inset.

sion is far less efficient in the latter case. Moreover, nearly half of all pulse energy is contained in the spectral wings that will be lost after final narrow-band filtering of the signal. Similar distortions in the spectrum of the pulse that experienced parabolic shaping are much less pronounced. The peak value of spectral density is orders of magnitude higher than its values at local satellite peaks.

As a result, we note that half-maximum of compressed spectrum of the pulse propagated through a *PS* element is $\Delta\omega = 0.336 \times 10^{12}$ s^{-1}, while its peak spectral density is $P_{max} = 4.41 \times 10^7$ W s^{-2} (curve *3*). At the same time, the corresponding values for compressed spectrum of the pulse that did not pass through a fiber with a decreasing with length dispersion are $\Delta\omega = 1.33 \times 10^{12}$ s^{-1} and $P_{max} = 1.09 \times 10^7$ W s^{-2} (curve *2*), respectively. Thus, preliminary propagation of the pulse through a *PS* element allows increasing the nonlinear spectral-shaping efficiency by nearly a factor of 4.

CONCLUSIONS

In the present work, we numerically investigated nonlinear spectral compression of a subpicosecond laser pulse of medium energy in a fiber-optic system. It is shown that the final shape of the envelope of the initial pulse is critically important for quality of final compression. In so doing, maximum degree of spectral compression is achieved for a parabolic shape of the pulse envelope.

A cascade model of the fiber-based spectral-compression system containing an element that ensures transformation of the pulse envelope toward a parabolic shape is proposed. It is demonstrated that, for values of parameters typical of standard optical single-mode fibers, the proposed cascade model affords increased quality of spectral compression (relative to the standard scheme). The proposed model can be used in a number of nonlinear-optical applications, such as frequency conversion and generation of harmonics.

ACKNOWLEDGMENTS

This work was supported by the Ministry of Education and Science of the Russian Federation (state assignment no. 3.3889.2017) and the Russian Science Foundation (projects nos. 16-42-02012 and 17-7210135).

REFERENCES

1. R. Wynands, O. Coste, C. Rembe, and D. Meschede, Opt. Lett. **20**, 1095 (1995).
2. R. G. Zaporozhchenko, Opt. Spectrosc. **95**, 976 (2003).
3. A. N. Tkachev and S. I. Yakovlenko, Quantum Electron. **33**, 581 (2003).
4. G. N. Makarov, Phys. Usp. **58**, 670 (2015).
5. K. H. Ylä-Jarkko and A. B. Grudinin, IEEE Photon. Technol. Lett. **15**, 191 (2003).

6. S. Singh and N. Singh, Prog. Electromagn. Res. **73**, 249 (2007).
7. R. H. Stolen and C. Lin, Phys. Rev. A **17**, 1448 (1978).
8. S. A. Planas, N. P. Mansur, C. B. Cruz, and H. L. Fragnito, Opt. Lett. **18**, 699 (1993).
9. M. J. Digonnet, *Rare-Earth-Doped Fiber Lasers and Amplifiers, Revised and Expanded,* Optical Science and Engineering (CRC, Boca Raton, FL, 2001).
10. A. Tünnermann, T. Schreiber, and J. Limpert, Appl. Opt. **49**, 71 (2010).
11. G. Agrawal, *Nonlinear Fiber Optics* (Academic, New York, 2007).
12. J. Fatome, B. Kibler, E. Andresen, H. Rigneault, and C. Finot, Appl. Opt. **51**, 4547 (2012).
13. S. Boscolo, F. Chaussard, E. Andresen, H. Rigneault, and C. Finot, Opt. Laser Technol. **99**, 301 (2018). doi 10.1016/j.optlastec.2017.08.033
14. I. O. Zolotovskii, D. A. Korobko, A. A. Sysoliatin, and A. A. Fotiadi, J. Russ. Laser Res. **37**, 448 (2016).
15. A. Monmayrant, S. Weber, and B. Chatel, J. Phys. B: At., Mol. Opt. Phys. **43**, 103001 (2010).
16. T. Hirooka and M. Nakazawa, Opt. Lett. **29**, 498 (2004).
17. I. O. Zolotovskii, D. A. Korobko, O. G. Okhotnikov, D. I. Sementsov, A. A. Sysolyatin, and A. A. Fotiadi, Opt. Spectrosc. **114**, 260 (2013).
18. U. G. Akhmetshin, V. A. Bogatyrev, A. K. Senatorov, A. A. Sysolyatin, and M. G. Shalygin, Quantum Electron. **33**, 265 (2003).

Translated by I. Shumai